Archives of Virology
https://doi.org/10.1007/s00705-021-05187-8

ORIGINAL ARTICLE

Detection of white spot syndrome virus in seafood samples using a magnetosome-based impedimetric biosensor

Sumana Sannigrahi[1] · Shiva Kumar Arumugasamy[2] · Jayaraman Mathiyarasu[3] · R. Sudhakaran[4] · K. Suthindhiran[5]

Received: 18 January 2021 / Accepted: 7 June 2021

Abstract

White spot syndrome virus (WSSV) is a significant threat to the aquaculture sector, causing mortality among crabs and shrimps. Currently available diagnostic tests for WSSV are not rapid or cost-effective, and a new detection method is therefore needed. This study demonstrates the development of a biosensor by functionalization of magnetosomes with VP28-specific antibodies to detect WSSV in seafood. The magnetosomes (1 and 2 mg/ml) were conjugated with VP28 antibody (0.025–10 ng/µl), as confirmed by spectroscopy. The magnetosome-antibody conjugate was used to detect the VP28 antigen. The binding of antigen to the magnetosome-antibody complex resulted in a change in absorbance. The magnetosome-antibody-antigen complex was then concentrated and brought near a screen-printed carbon electrode by applying an external magnetic field, and the antigen concentration was determined using impedance measurements. The VP28 antigen (0.025 ng/µl) bound more efficiently to the magnetosome-VP28 antibody complex (0.025 ng/µl) than to the VP28 antibody (0.1 ng/µl) alone. The same assay was repeated to detect the VP28 antigen (0.01 ng/µl) in WSSV-infected seafood samples using the magnetosome-VP28 antibody complex (0.025 ng/µl). The WSSV in the seafood sample was also drawn toward the electrode due to the action of magnetosomes controlled by the external magnetic field and detected using impedance measurement. The presence of WSSV in seafood samples was verified by Western blot and RT-PCR. Cross-reactivity assays with other viruses confirmed the specificity of the magnetosome-based biosensor. The results indicate that the use of the magnetosome-based biosensor is a sensitive, specific, and rapid way to detect WSSV in seafood samples.

Introduction

White spot syndrome virus (WSSV) poses a significant threat to the aquaculture industry globally. WSSV is a large DNA virus (210–420 nm × 70–167 nm) that contains 35 different envelope proteins [1, 2]. It infects all of the life

Handling Editor: Kalpana Agnihotri.

✉ K. Suthindhiran
ksuthindhiran@vit.ac.in; sudhindhira@gmail.com

Sumana Sannigrahi
sumanasannigrahi11@gmail.com

Shiva Kumar Arumugasamy
shiva.cva16@outlook.com

Jayaraman Mathiyarasu
al_mathi@yahoo.com

R. Sudhakaran
2sudha@gmail.com; sudhakaran.r@vit.ac.in

[1] Marine Biotechnology and Bioproducts Lab, School of Bio Sciences and Technology, VIT, Vellore, Tamil Nadu 632014, India

[2] Electrodics and Electrocatalysis Division, CSIR-Central Electrochemical Research Institute, Karaikudi, Tamil Nadu 630003, India

[3] Electrodics and Electrocatalysis Division, CSIR-Central Electrochemical Research Institute, Karaikudi, Tamil Nadu 630003, India

[4] Aquaculture Biotechnology Laboratory, School of Biosciences and Technology, Vellore Institute of Technology, Vellore, Tamil Nadu 632014, India

[5] Marine Biotechnology and Bio Products Lab, School of Bio Sciences and Technology, Vellore Institute of Technology, Vellore, Tamil Nadu 632014, India

Published online: 03 August 2021

stages of *Penaeus monodon* and *Marsupenaeus japonicas* shrimp and other crustaceans, causing mortality within 3–10 days [3–8]. VP28 plays a significant role in the initial steps of systemic WSSV infection as an envelope protein and as an attachment protein by binding the virus to shrimp cells, thereby helping the virus to enter the cytoplasm [9, 10]. This virus mainly infects the stomach, gills, and cuticular epidermis of shrimps and suppresses their ability to eliminate the free radicals present in the cell, resulting in oxidative stress and death [11]. The Indian seafood export market is strongly affected by WSSV [12, 13].

Several techniques, including plaque assay, protein assay, quantitative polymerase chain reaction (qPCR), RT-PCR, ELISA, and far-Western blotting, have been used for the detection of WSSV [14–19]. However, these techniques can only be performed in a laboratory by professionals, and they are laborious [20].

Biosensors involve simple methodology and can provide high specificity and sensitivity in diagnosis. Enzymatic biosensors or immune sensors are used for the detection of microorganisms such as *Escherichia coli*, *Salmonella*, and *Staphylococcus aureus*, as well as pesticides and herbicides [21, 22]. However, the major drawbacks are a lack of stability and improper immobilization of the enzyme on the surface of the sensor. Nanoparticle-based biosensors are gaining attention due to their large specific surface area, ability to immobilize biomolecules, catalyze electrochemical reactions, and increase the transfer of electrons between electrode surfaces and proteins [23, 24]. However, the variable size range and toxicity of nanoparticles are major drawbacks of this technique [25]. Furthermore, the use of linker molecules for the attachment of biomolecules has increased the complexity of the nanoparticle technique [26].

To further improve the efficiency and simplicity of biosensors, biogenic nanoparticles can be used instead of chemically synthesized nanoparticles. Magnetosomes are magnetic iron mineral particles with a diameter of 35-120 nm that are synthesized by magnetotactic bacteria. They are Fe^{3+} [Fe^{2+}, Fe^{3+}] O_4 particles that are formed through genetically controlled biomineralization in all magnetotactic bacteria [27, 28]. Magnetosomes have a lipid bilayer, 58-65% of which is composed of phospholipids and 50% of which is composed of phosphatidylethanolamine, which provides an outward-facing amine group [29, 30]. Magnetosomes have a number of useful properties, including a narrow grain size distribution, chemical purity of magnetite crystals, the perfection in the crystal lattice and particle arrangement in chains, cubo-octahedral shape, high stability, and non-toxicity [31]. They have the advantage that their membrane provides better dispersion and handling properties than magnetic particle conjugates [32]. These properties have allowed the development of highly sensitive chemiluminescence enzyme immunoassays through the chemical coupling of antibodies to the magnetosome surface [33]. In this study, magnetosomes were conjugated with VP28 antibody without any linker molecules and used to detect the VP28 antigen of WSSV in infected seafood samples.

Materials and methods

Chemicals and reagents

The chemicals used in this study were obtained from HiMedia Laboratories, India. The primary antibody (VP28-specific IgG) and secondary antibody (goat anti-rabbit IgG) labeled with horseradish peroxidase (HRP) were purchased from GeNei Products from Merck India, Bioscience. 2, 2' azino-(di-3-ethybenzthiozoline sulfonic acid (ABTS) was purchased from SRL Limited, India.

Instrumentation

Magnetosomes were ultrasonicated using an Ultrasonic Cleaner EN30VS, (Life Care, India). Quantitation of antibody binding to magnetosomes and ELISA were carried out using a 96-well plate reader (LIMR96, Lark Innovative Fine Tecknowledge, India). The UV-vis spectrophotometer was obtained from ELICO, India. SDS-PAGE was performed using an apparatus purchased from MEDOX SDS, India. Membrane transfer was performed using a semi-dry blot apparatus (Benchtop, India). A one-step reverse transcriptase kit from Invitrogen (USA) was used for PCR amplification in an Eppendorf thermal cycler (Belgium). Impedance responses were measured using a PARSTAT electrochemical workstation (Princeton Applied Research) at room temperature in Fe $(CN)_6^{3-}/^{4-}$electrolyte with an RRPE1002C screen-printed carbon electrode (SPCE), which acted as a working electrode, a counter electrode, and a reference electrode (Pine Research Instrumentation, Durham, USA).

Extraction and immobilization of magnetosomes

Magnetosomes were extracted from *Magnetospirillum* sp. RJS1 [34] and examined by electron microscopy [35]. The magnetosome-VP28 antibody complex was prepared as described previously, with modifications [35]. Briefly, 1-2 mg of magnetosomes was ultra-sonicated at 20 kHz for 10 min in phosphate-buffered saline (PBS). For the binding reaction, 100 µl of VP28 antibody (0.01–10 ng/µl) was added to 900 µl of magnetosome solution. After incubation at 4°C for 24 hours, the tubes containing magnetosome-antibody complex were attached to a neodymium magnet and washed 10-12 times in PBS with 1% bovine serum albumin (BSA). The absorbance was measured at 630 nm.

Sample collection and VP28 antigen extraction

Freshwater crabs (*Paratelphusa hydrodomous*) were collected from a rice field in Vellore, India, and maintained in the laboratory at room temperature (27–30 °C) for seven days. The crabs were then checked for signs of WSSV infection, and six different sets of healthy crabs were divided into two separate groups: control (healthy) and test (WSSV-infected). The experiments were carried out in triplicate. Crabs in the test group were injected with WSSV [36, 37], and the first set of crabs were sacrificed after seven days, and antigen was collected from infected gill tissue samples [38]. Briefly, the tissues were homogenized in NaCl-Tris-EDTA (NTE) buffer (0.2 M NaCl, 0.02 M Tris-HCl, and 0.02 EDTA, pH 7.4) and then centrifuged at 3000 × *g* for 20 min at 4°C. The supernatant was collected and centrifuged again (8000 × *g*, 30 min, 4°C). The final supernatant was separated and then passed through a 0.4-µm filter. The total protein content in the filtrate was determined [39], and the sample was stored at –20°C.

Preparation of magnetosome-VP28 antibody-VP28 antigen complexes

The protocol of Sannigrahi et al. was followed [35]. In summary, purified VP 28 antigen (0.1 ng/µl) was coated (100 µl) onto a 96-well plate, which was incubated overnight at 4 °C. The wells were then washed six times with PBS-Tween 20 (PBST), and magnetosome-VP28 antibody complexes (0.01-10 ng/µl), 100 µl of each concentration, were added to the washed wells, and the plate was incubated at room temperature for 1 h. After incubation, the magnetosome-VP28 antibody-VP28 antigen complex was concentrated in the plate using a magnet, followed by washing three times with PBST to remove unbound anti-VP28 antibody. The absorbance of the magnetosome-VP28 antibody complex with antigen was then measured at 630 nm and compared with the absorbance of the magnetosomes without VP28 antibody and VP28 antigen.

Enzyme-linked immunosorbent assay (ELISA)

ELISA to screen VP28 antigen

Magnetosome-based ELISA was performed as described by Sannigrahi et al. [35]. A magnetosome-VP28 antibody complex was used in the assay. The VP28 antigen (0.1 ng/µl) was coated on the wells. Next, different concentrations of magnetosome-VP28 antibody complexes (0.025–10 ng/µl) were added to the VP28 antigen-coated wells. After washing with PBS, 100 µl of secondary antibody-HRP (50 ng/ml) was added to the wells, and the plate was incubated for 1 h at room temperature. Then, VP28 antigen-magnetosome-VP28 antibody-secondary antibody complex was concentrated in the wells using a bar magnet. ABTS substrate (100 µl) was added to the complex, and absorbance at 405 nm was recorded.

In order to determine the lowest measurable concentration of VP28 antigen, various concentrations of VP28 antigen (0.025–10 ng/µl) were prepared in carbonate-bicarbonate buffer, and 100 µl of each concentration was coated onto the wells in triplicate. Next, 100 µl of (1 or 2 mg/ml) magnetosome-VP28 antibody complex (0.05 ng/µl) and secondary antibody-HRP (50 ng/ml) were added simultaneously to the VP28 antigen-coated wells as described above. Finally, ABTS was added, and absorbance was recorded at 405 nm.

Screening of VP28 antigen from an infected tissue sample

This protocol was modified from earlier publications [38, 40]. The second set of crabs were sacrificed after seven days, and infected tissues were collected. One gram of infected crab gill tissue sample was suspended in 10 ml of NaCl-Tris EDTA buffer and ground manually. The homogenized sample was frozen and thawed three times and stored for further use. The prepared tissue suspension was mixed with different concentrations of magnetosome-VP28 antibody complex (0.025–10 ng/µl) in a 1:1 ratio and incubated for 48 h at 4 °C. The magnetosome-VP28 antibody-VP28 antigen complex was concentrated in the 96-well plate using a bar magnet and incubated overnight at 4 °C. Then, 100 µl of 1% BSA was added to the wells, and the plate was washed 9-10 times. ELISA was performed using HRP-conjugated secondary antibody (50 ng/ml). ABTS substrate was added, and the absorbance was measured at 405 nm.

Impedance-based electrochemical studies

Impedance-based spectroscopy for magnetosome-VP28 antibody coupling

To examine the binding of magnetosomes with VP28 antibodies, impedance-based studies with SPCEs were performed as described by Sannigrahi et al., with modifications [35]. To activate the surface of the SPCEs, they were treated with 0.1 M Na_2CO_3 at 1.2 V. The treated SPCEs were loaded with 10 µl of VP28 antibody (1 ng/µl). The measurements were carried out in electrolyte (1 mM of $K_4[Fe(CN)_6]$ and $K_3[Fe(CN)_6]$ in 0.1 M KNO_3 prepared using 10 mM PBS). The open-circuit potential was implemented for impedance response recorded against imaginary *vs*. real components (0.1 Hz-100 kHz) with 10 mV amplitude. The data were then processed using ZVIEW software. The impedance measurements for the VP28 antibody (0.025–0.1 ng/µl) and magnetosome-VP28 antibody complex were carried out in the same manner.

Detection of magnetosome-VP28 antibody-VP28 antigen complexes

To detect the binding of VP28 antigen with magnetosome (2 mg/ml)-VP28 antibody complexes, impedance measurements were taken using a PARSTAT electrochemical workstation (Princeton Applied Research). The magnetosome (2 mg/ml)-VP28 antibody complexes (0.025 ng/µl) were coated on SPCEs and concentrated on the working electrode using a bar magnet. Then, 10 µl of VP28 antigen (0.01-1 ng/µl) was added to the concentrated magnetosome-VP28 antibody complex. The SPCEs were incubated at 37 °C for 60 min, followed by washing with PBS and deionized water.

Detection of WSSV in electrochemical impedance spectroscopy (EIS)

WSSV was also detected in serum samples of crabs. The third set of crabs (control and test) were sacrificed after seven days, and tissues were suspended in 10 ml of NaCl-Tris EDTA buffer and ground manually with a mortar and pestle. Homogenized tissues from both groups were frozen and thawed three times and stored for further use. The infected sample was diluted 10^{-1}- to 10^{-7}-fold in serum dilution. Then, 100 µl of magnetosome-VP28 antibody complex was added to 100 µl of WSSV for each dilution. An uninfected control group was also included. The mixtures were incubated at room temperature for 30 min, and a bar magnet was attached to magnetically wash the complexes. The complexes were attached to the SPCEs, and impedance was measured for each dilution and control to confirm the positive detection.

SDS-PAGE and Western blot analysis

The presence of WSSV was also detected by SDS-PAGE and Western blot [41]. The fourth and fifth sets of crabs were sacrificed on the first and seventh day, respectively. Healthy and infected tissues from gills and heads were collected from both sets. Protein was extracted from the infected tissue samples using lysis buffer. The total protein concentration was measured using a spectrophotometer. The protein was then denatured in SDS-containing buffer for SDS-PAGE. Stacking and separating gels were prepared, and SDS-PAGE was performed. For Western blot analysis, the proteins separated by SDS-PAGE were transferred onto a nitrocellulose membrane using a dry blotter. Membranes were blocked with 1% BSA for 2 h and then washed with PBS. Immunodetection was performed by incubating the membrane with VP28 antibody (0.1 µg/µl) overnight at room temperature. Subsequently, HRP-conjugated secondary antibody (0.1 µg/µl) was added to the membrane for 2-3 h, and detection was performed with 5-bromo 4-chloro 3-indol phosphate (BCIP) and nitro blue tetrazolium (NBT).

Reverse transcription polymerase chain reaction (RT-PCR)

The protocol was modified from Reddy et al. [42]. The sixth set of both healthy and WSSV-infected crabs were sacrificed after the seventh day, and tissues from gills and heads were collected. The total RNA was extracted from healthy and infected tissues. Complementary DNA was synthesized from 1 µg of total RNA using a one-step reverse transcriptase kit as per the instructions in the user manual and used as a template for analysis of expression of the VP28 gene. The cycling conditions included initial denaturation at 95 °C for 5 min, followed by 35 cycles of denaturation at 95 °C for 30 s, annealing at 50 °C for 30 s, and extension at 72 °C for 30 s, and a final extension step at 72 °C for 10 min. The PCR product was subjected to electrophoresis in a 1.0% agarose gel and viewed using an ultraviolet transilluminator (Table 1).

Cross-reactivity of VP28 antibody

VP28 antigen along with four other non-VP28 antigens: *Lactococcus garvieae* (LC), *Enterocytozoon hepatopenaei* (EHP), *Edwardsiella tarda* (ET), and infectious hypodermal and hematopoietic necrosis virus (IHHNV) were tested with VP28 antibody in ELISA. VP28 antigen (1 ng/µl) and non-VP28 antigen (1 ng/µl) were coated onto the plate. VP28 antibody (1 ng/µl) and HRP-conjugated secondary antibody (50 ng/ml) were used in this assay.

The cross-reactivity of the magnetosome-VP28 antibody complex with WSSV and other seafood pathogens (LC, EHP, ET, and IHHNV) was also confirmed by EIS. Five different sets of crabs were infected in triplicate with five different pathogens. The crabs were sacrificed and infected tissues were collected. Each set of tissue samples was suspended in 10 ml of NaCl-Tris EDTA buffer and ground manually. The homogenized sample sets were frozen and thawed three times and stored for further use. A control sample set (healthy crab without infection) was also homogenized.

Table 1 Oligonucleotide primers used for RT-PCR

Primer name	Sequence (5'- 3')	Annealing temperature	Product size
VP28 RT-F	CCA AGA CCA TCG AAA CCC AC	60ºC	200 bp
VP28 RT-R	TGC GGA TCT TGA TTT TGC CC		

The prepared tissue suspension (100 µl) from each seafood pathogen and control was incubated at room temperature for 30 min with 100 µl of the magnetosome-VP28 antibody complex. A bar magnet was attached to magnetically wash the complexes, and EIS was performed after concentrating the complexes on the SPCEs.

Results

Conjugation of magnetosomes with VP28 antibodies

The binding of VP28 antibodies directly to the surface of the magnetosomes was confirmed using absorbance spectroscopy. The magnetosomes (1 mg/ml) coupled with VP28 antibody (0.2 ng/µl) had higher absorbance (0.166) than that of magnetosomes (0.089) or VP28 antibodies (0.032) alone (Fig. 1a). Likewise, magnetosomes (2 mg/ml) coupled with VP28 antibodies (0.2 ng/µl) also showed higher absorbance (0.180) than that of magnetosomes (0.096) or VP28 antibodies (0.032) alone (Fig. 1b). This indicates that the VP28 antibodies were bound to the magnetosomes.

Detection of VP 28 antigen without magnetosomes

The VP 28 antigen concentration (0.1–100 ng/µl) was determined by ELISA in the absence of magnetosomes. The VP28 antibody (0.01–10 ng/µl) and HRP-conjugated secondary antibody (0.01–10 ng/µl) were implemented in the assay. The optimal concentrations of VP28 antigen (0.1 ng/µl, Fig. 2a), VP28 antibody (0.1 ng/µl, Fig. 2b), and secondary antibody-HRP (0.025 ng/µl, Fig. 2c) were used in subsequent experiments.

Coupling of VP28 antigen with magnetosome-VP28 antibody complex

The average absorbance of VP28 antigen coupled with magnetosome (1 mg/ml)-VP28 antibody (0.2 ng/µl) complex (0.185) was higher than that of magnetosome (1 mg/ml)-VP28 antibody (0.2 ng/µl) complex (0.166) or VP28 antigen (0.045) alone (Fig. 3a). Likewise, VP28 antigen coupled with magnetosome (2 mg/ml)-VP28 antibody (0.2 ng/µl) complex (0.214) had higher absorbance than that of the components alone (magnetosome [2 mg/ml]-VP28 antibody [0.2 ng/µl] complex [0.180] or VP28 antigen [0.045]) (Fig. 3b).

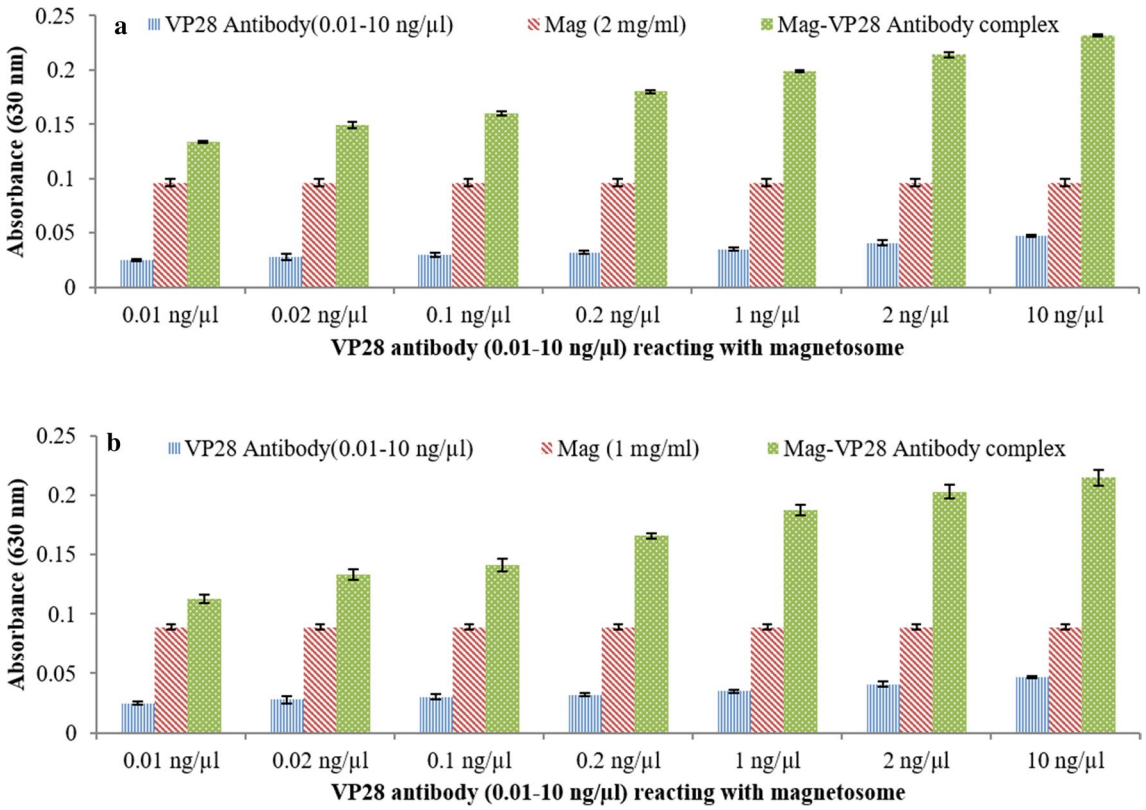

Fig. 1 **a** Absorption measurements to detect the coupling of VP28 antibody (0.01–10 ng/µl) with magnetosomes at 1 mg/ml. **b** Absorption measurements to detect the coupling of VP28 antibody (0.01–10 ng/µl) with magnetosome at 2 mg/ml

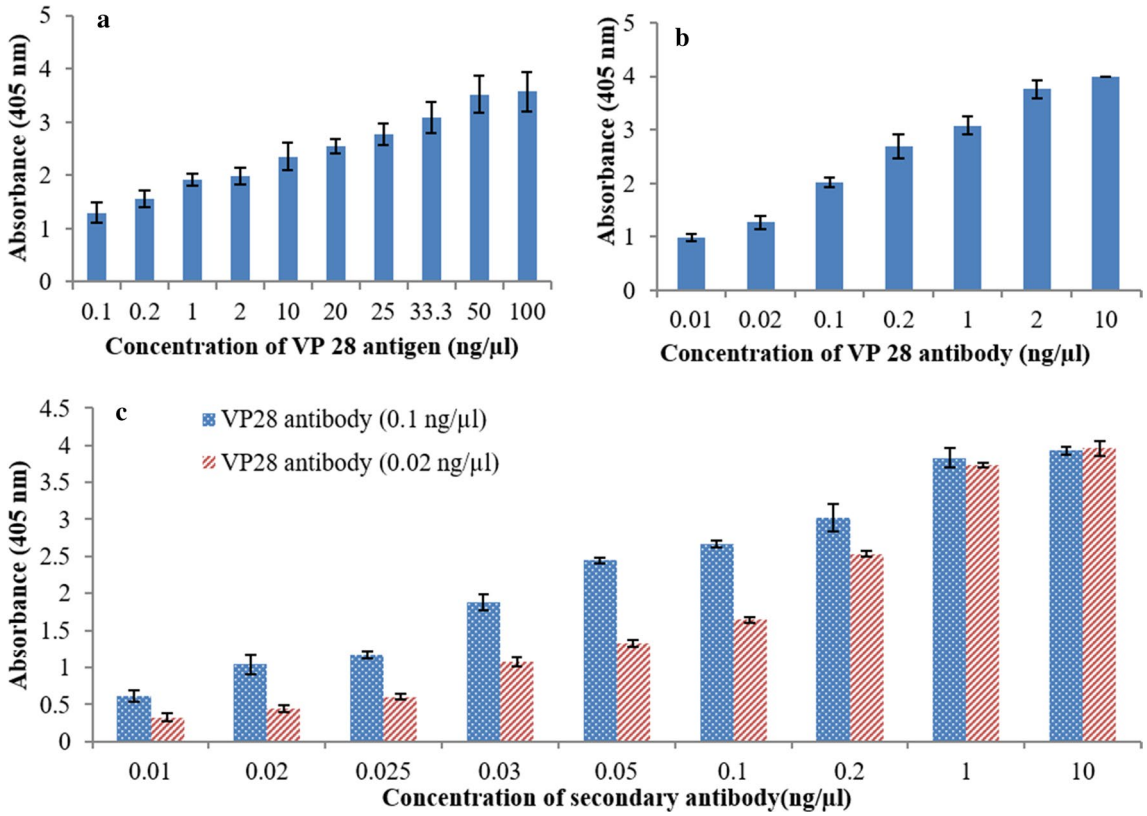

Fig. 2 **a** Colorimetric assay to optimize the VP28 antigen concentration (0.1-100 ng/µl). **b** Colorimetric assay to optimize the VP28 antibody concentration (0.01-10 ng/µl). VP28 antibody (0.1 ng/µl) was used to detect VP28 antigen (0.1 ng/µl). **c** Colorimetric assay to optimize the secondary antibody concentration (0.01-10 ng/µl) using VP28 antibody (0.1 ng/µl and 0.02 ng/µl).

ELISA using the magnetosome-VP28 antibody complex

Detection of VP28 antigen using magnetosome-VP28 antibody complex

Magnetosomes at two different concentrations, 1 mg/ml and 2 mg/ml, were used in the assay. The VP28 antigen (0.1 ng/µl) was effectively detected using (2 mg/ml)-VP28 antibody complex (0.025–1 ng/µl), (1 mg/ml)-VP28 antibody complex (0.025–1 ng/µl), and VP28 antibody (0.025–1 ng/µl) alone (Fig. 4a). However, an absorbance difference (0.802) was observed between the magnetosome (2 mg/ml)-VP28 antibody complex and VP28 antibody alone at 0.025 ng/µl concentration. This indicated that magnetosomes coupled with a lower concentration of VP28 antibody (0.025 ng/µl) could detect the VP28 antigen (0.1 ng/µl) more efficiently than the antibody (0.1 ng/µl) alone at high concentration.

$$\%Cost\ effectivity = \frac{Conc.\ of\ control - Conc.\ of\ test}{Conc.\ of\ control} \times 100 \quad (1)$$

$$\%Cost\ effectivity = \frac{0.1 - 0.025}{0.1} \times 100$$

$$\%Cost\ effectivity = 75$$

The magnetosome-based ELISA produces a 75% cost-effective approach compared to the conventional assay to detect the VP28 antigen. Furthermore, at a concentration of 1 mg/ml, the magnetosome complex containing 0.05 ng VP28 antibody per µl also showed higher absorbance (1.413) than VP28 antibody alone at a concentration of 0.05 ng/µl (1.03).

VP28 antigen at various concentrations (0.025–10 ng/µl) was also detected in the magnetosome-based ELISA (Fig. 4b). The VP28 antigen at a concentration of 0.1 ng/µl was more efficiently detected using the magnetosome (2 mg/ml)-VP28 antibody (0.05 ng/µl) complex (absorbance, 1.1775) than with VP28 antibody (0.05 ng/µl) alone (absorbance, 0.91). The 1 mg/ml concentration of magnetosome coupled with VP28 antibody (0.05 ng/µl) also detected (absorbance, 0.931) the VP28 antigen (0.1 ng/µl). Further, the magnetosome (2 mg/ml)-VP28 antibody complex

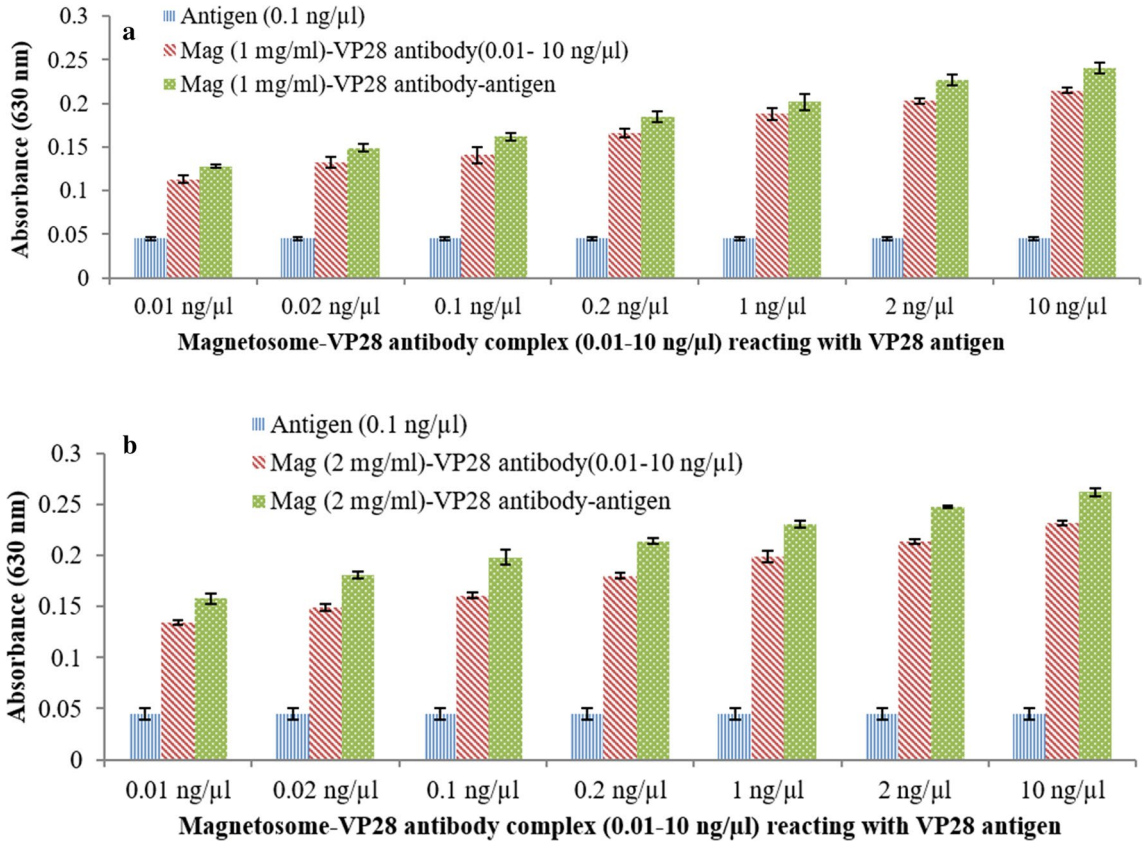

Fig. 3 **a** Absorption measurements at 630 nm for immunoassay to detect the coupling of VP28 antigen (0.1 ng/µl) with magnetosome (1 mg/ml)–VP28 antibody (0.01–10 ng/µl) complex. **b** Absorption measurements at 630 nm for immunoassay to detect the coupling of VP28 antigen (0.1 ng/µl) with magnetosome (2 mg/ml)–VP28 antibody (0.01–10 ng/µl) complex

detected VP28 antigen (0.025 ng/µl) with an absorbance value of 0.666.

ELISA to detect VP28 antigen extracted from the tissue samples

Magnetosomes at two different concentrations (1 and 2 mg/ml) coupled with the various concentrations of VP28 antibody (0.025–10 ng/µl) effectively detected the VP28 antigen extracted from the tissue samples (Fig. 5). Magnetosomes (2 mg/ml) conjugated with VP28 antibody (0.025 ng/µl) showed sufficient absorbance (0.325) for detecting the VP28 antigen in a tissue sample. Similarly, magnetosomes (1 mg/ml) conjugated with VP28 antibody (0.025 ng/µl) show sufficient absorbance (0.321) for detecting the VP28 antigen.

EIS using magnetosome-VP28 antibody complex

Binding of VP28 antibody to magnetosomes

The bare response of SPCE was 278 Ω charge transfer resistance (R_{CT}), while it was 505 Ω R_{CT} when VP28 antibody (0.025 ng/µl) was used for coating (Fig. 6a, Table 2). It was further noted that the resistance on the electrode surface kept increasing with increasing VP28 antibody concentration (0.03 ng/µl, 782 Ω; 0.05 ng/µl, 996 Ω; 0.1 ng/µl, 1068 Ω; 1 ng/µl, 1164 Ω). Similarly, when the magnetosome-VP28 antibody (0.025 ng/µl) complex (702 Ω) was coated onto the bare SPCE (257 Ω), a difference in resistance was evident (Fig. 6b, Table 3). Moreover, the electrode resistance increased with the concentration of magnetosome-VP28 antibody complex (0.03 ng/µl, 860 Ω; 0.05 ng/µl, 1035 Ω; 0.1 ng/µl, 1224 Ω; 1 ng/µl, 1640 Ω).

R_s, Solution resistance; Cdl, double-layer capacitance; R_{CT}, charge transfer resistance; Q, constant phase element; W, Warburg resistance; RSD, relative standard deviation

VP28 antigen interaction with magnetosome-VP28 antibody complex

The interaction of VP28 antigen with VP28 antibody as well as magnetosome-VP28 antibody complex was studied using impedance measurements (Fig. 6a and b). The impedance of the bare SPCE and VP28 antibody (0.025 ng/µl)

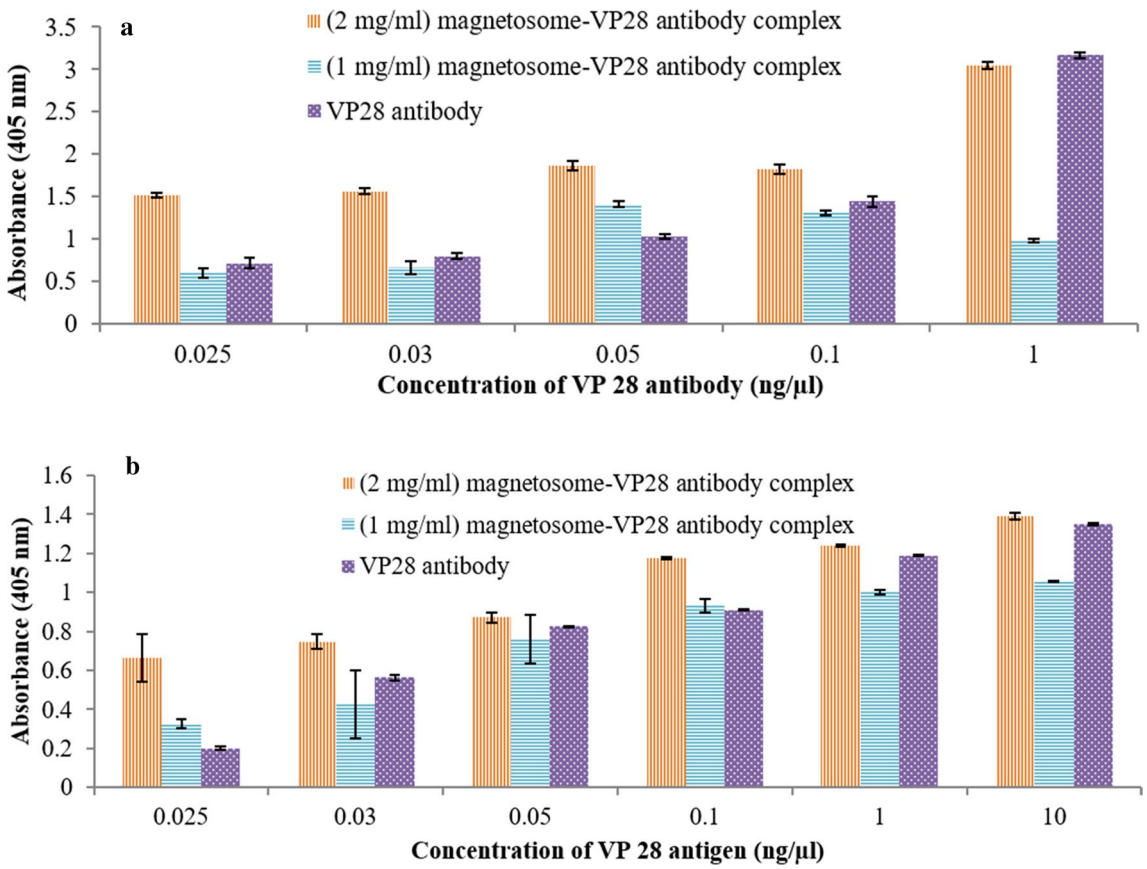

Fig. 4 **a** Colorimetric immunoassay to detect VP28 antigen (0.1 ng/µl) using magnetosome (2 mg/ml)–VP28 antibody complex, magnetosome (1 mg/ml)–VP28 antibody complex, and VP28 antibody (0.025-1 ng/µl). **b** Colorimetric immunoassay to detect VP28 antigen in various concentrations (0.025-10 ng/µl) using magnetosome (2 mg/ml)–VP28 antibody (0.05 ng/µl) complex, magnetosome (1 mg/ml)–VP28 antibody (0.05 ng/µl) complex, and VP28 antibody (0.05 ng/µl)

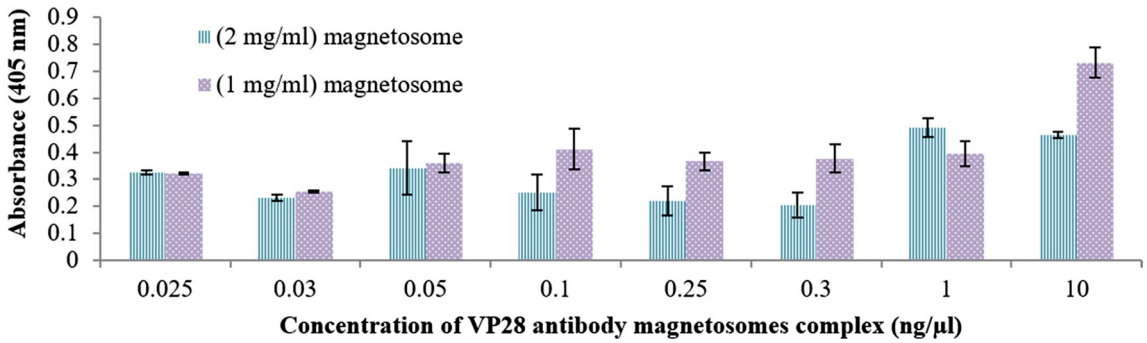

Fig. 5 Colorimetric immunoassay to detect VP28 antigen extracted from the tissue samples

was recorded as 337 Ω and 624 Ω, respectively. The impedance for VP28 antigen (0.01 ng/µl) was higher (846 Ω) when it interacted with the VP28 antibody. Furthermore, when increasing concentrations of VP28 antigen interacted with the VP28 antibody, an increase in resistance was observed (0.03 ng/µl, 981 Ω; 0.05 ng/µl, 1029 Ω; 0.1 ng/µl, 1194 Ω; 1 ng/µl, 1480 Ω; Table 4).

The interaction of magnetosome-VP28 antibody complex with VP28 antigen also showed a similar response. The combined resistance of magnetosome-VP28 antibody (0.025 ng/µl) complex with VP28 antigen at 0.01 ng/µl (926 Ω) was higher than magnetosome-VP28 antibody (0.025 ng/µl) alone (794 Ω). The other concentration of VP28 antigen (0.03-1 ng/µl) also interacted with

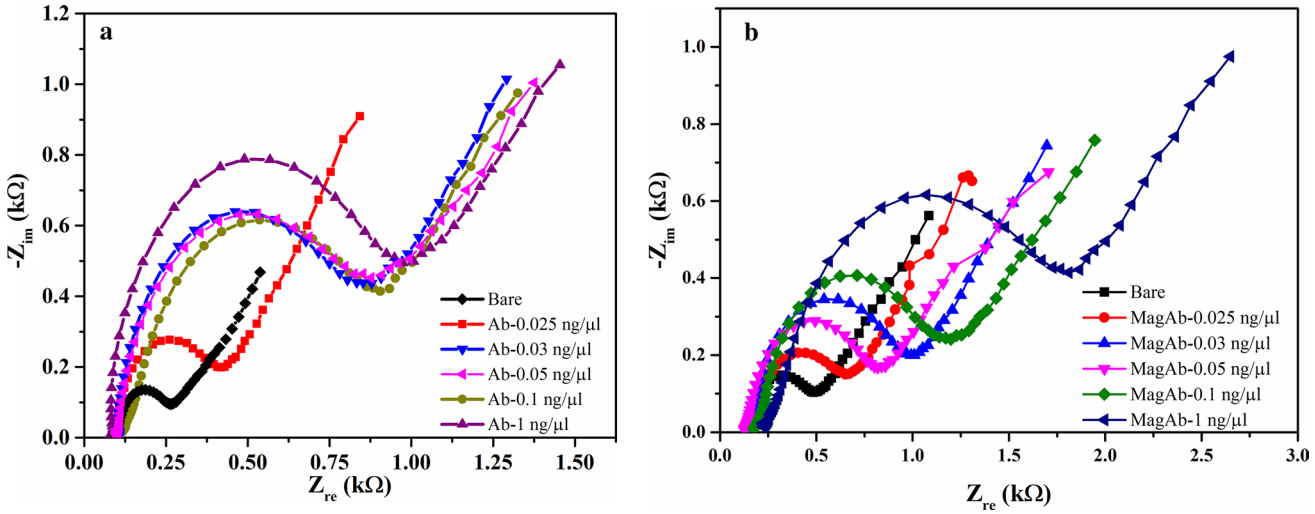

Fig. 6 **a** Impedance-based measurements for the various concentrations of VP28 antibody (0.025-1 ng/µl). **b** Impedance-based measurements for the various concentrations of magnetosome-VP28 antibody (0.025-1 ng/µl) complex

Table 2 Impedance response at various VP28 antibody concentrations (0.025-1 ng/µl)

Concentration of Ab	R_S (Ω)	C_{dl} (µF)	R_{CT} (Ω)	Q	W (Ω)	RSD%
Bare	114	1.04	278	0.56	1.04×10^{-5}	1.64
0.025 ng/µl	108	1.25	505	0.89	3.66×10^{-5}	1.32
0.03 ng/µl	112	1.56	782	0.71	2.81×10^{-5}	2.20
0.05 ng/µl	109	1.79	996	0.92	3.05×10^{-5}	2.62
0.1 ng/µl	104	1.92	1068	0.86	2.91×10^{-5}	2.45
1 ng/µl	115	2.08	1164	0.67	3.81×10^{-5}	2.08

Table 3 Impedance response of various magnetosome-VP28 antibody concentrations (0.025-1 ng/µl)

Concentration of MagAb	R_S (Ω)	C_{dl} (µF)	R_{CT} (Ω)	Q	W (Ω)	RSD%
Bare	220	2.12	257	0.45	1.28×10^{-5}	1.24
0.025 ng/µl	225	2.54	702	0.62	2.05×10^{-5}	1.62
0.03 ng/µl	243	2.68	860	0.84	2.61×10^{-5}	1.49
0.05 ng/µl	220	2.73	1035	0.76	2.45×10^{-5}	2.03
0.1 ng/µl	214	2.96	1224	0.82	2.86×10^{-5}	2.24
1 ng/µl	245	3.05	1640	0.54	3.04×10^{-5}	2.98

Table 4 Impedance response of VP28 antigen (0.01-1 ng/µl) with VP28 antibody (0.025 ng/µl)

Concentration of Ab-Ag	R_S (Ω)	C_{dl} (µF)	R_{CT} (Ω)	Q	W (Ω)	RSD%
Bare	160	2.28	337	0.36	1.08×10^{-5}	1.04
Ab 0.025 ng/µl	175	2.08	624	0.52	1.24×10^{-5}	1.43
Ab-Ag 0.01 ng/µl	185	2.64	846	0.89	1.54×10^{-5}	1.26
Ab-Ag 0.03 ng/µl	203	2.87	981	0.54	1.76×10^{-5}	1.78
Ab-Ag 0.05 ng/µl	190	2.52	1029	0.86	1.89×10^{-5}	1.89
Ab-Ag 0.1 ng/µl	194	2.86	1194	0.91	2.04×10^{-5}	1.92
Ab-Ag 1 ng/µl	185	2.94	1480	0.72	2.26×10^{-5}	2.09

magnetosome-VP28 antibody (0.025 ng/µl) complex in a similar way (0.03 ng/µl, 1071; 0.03 ng/µl, 1214; 0.03 ng/µl, 1694; 0.03 ng/µl, 1986; Table 5). The linear correlation for both VP28 antibody and magnetosome-VP28 antibody interacting with VP28 antigen was found to be statistically significant (Fig. 7).

Detection of WSSV

It can be seen from Fig. 8 that the bare SPCE exhibited a low R_{CT} of 396 Ω. On modifying the electrode with magnetosome-VP28 antibody (0.025 ng/µl) complex with serum, a small semicircle was observed with R_{CT} of 850 Ω. Then,

Table 5 Impedance response of VP28 antigen (0.01-1 ng/µl) with magnetosome-VP28 antibody complex (0.025 ng/µl)

Concentration of MagAb-Ag	R_S (Ω)	C_{dl} (µF)	R_{CT} (Ω)	Q	W (Ω)	RSD%
Bare	270	1.96	340	0.48	0.97×10^{-5}	2.64
MagAb 0.025 ng/µl	285	2.43	794	0.67	1.56×10^{-5}	1.98
MagAb-Ag 0.01 ng/µl	287	2.57	926	0.82	1.89×10^{-5}	2.54
MagAb-Ag 0.03 ng/µl	273	2.87	1071	0.74	2.06×10^{-5}	2.06
MagAb-Ag 0.05 ng/µl	260	2.64	1214	0.48	2.98×10^{-5}	1.78
MagAb-Ag 0.1 ng/µl	284	2.73	1694	0.87	3.04×10^{-5}	2.67
MagAb-Ag 1 ng/µl	275	2.58	1986	0.98	3.46×10^{-5}	2.98

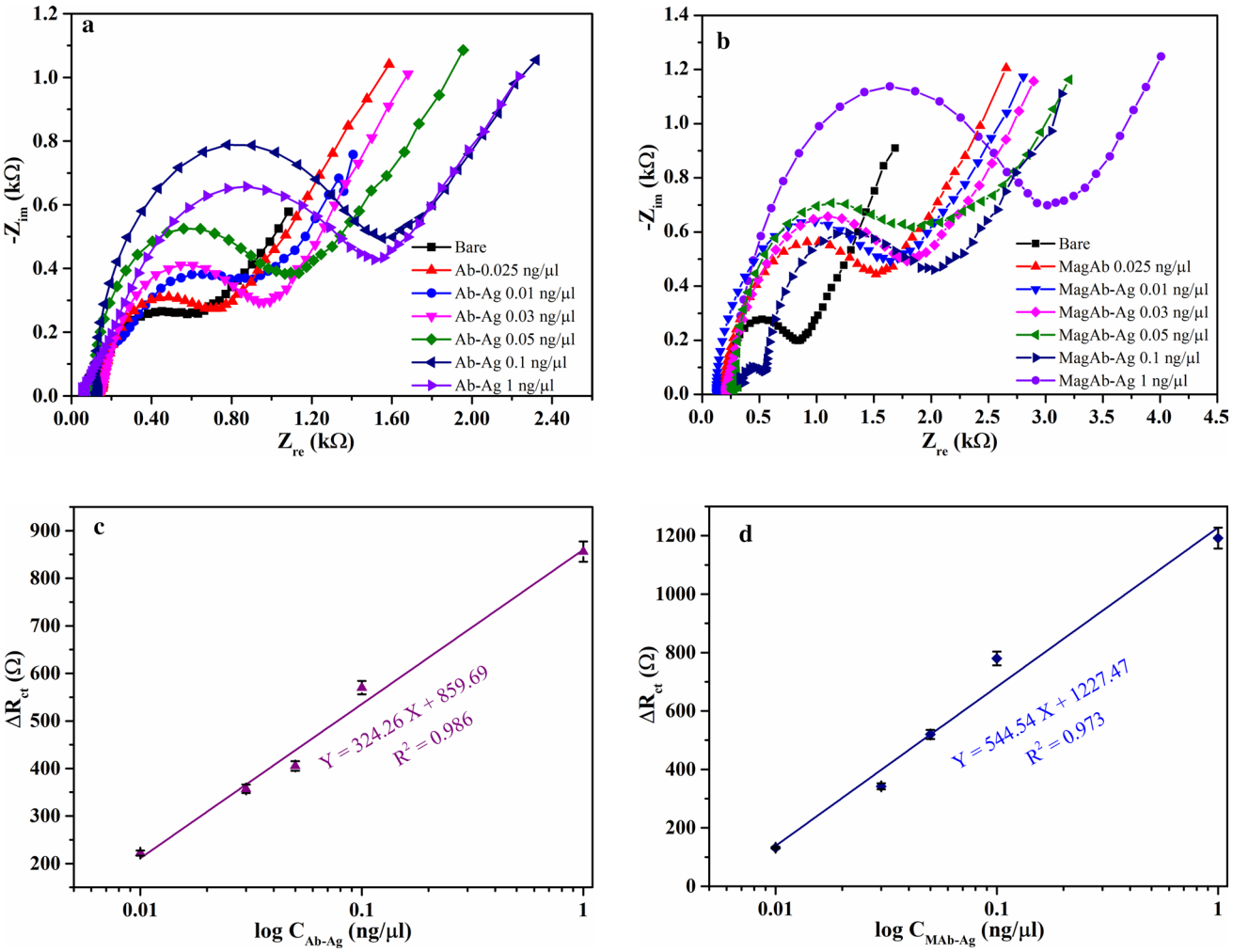

Fig. 7 (a) Impedance-based measurements for various concentrations of VP28 antigen (0.01-1 ng/µl) with VP28 antibody (0.025 ng/µl). (b) Impedance-based measurements for various concentrations of VP28 antigen (0.01-1 ng/µl) with magnetosome-VP28 antibody (0.025 ng/µl) complex. (c) Linear plot for the VP28 antibody-antigen interaction. (d) Linear plot for the magnetosome-VP28 antibody-antigen interaction

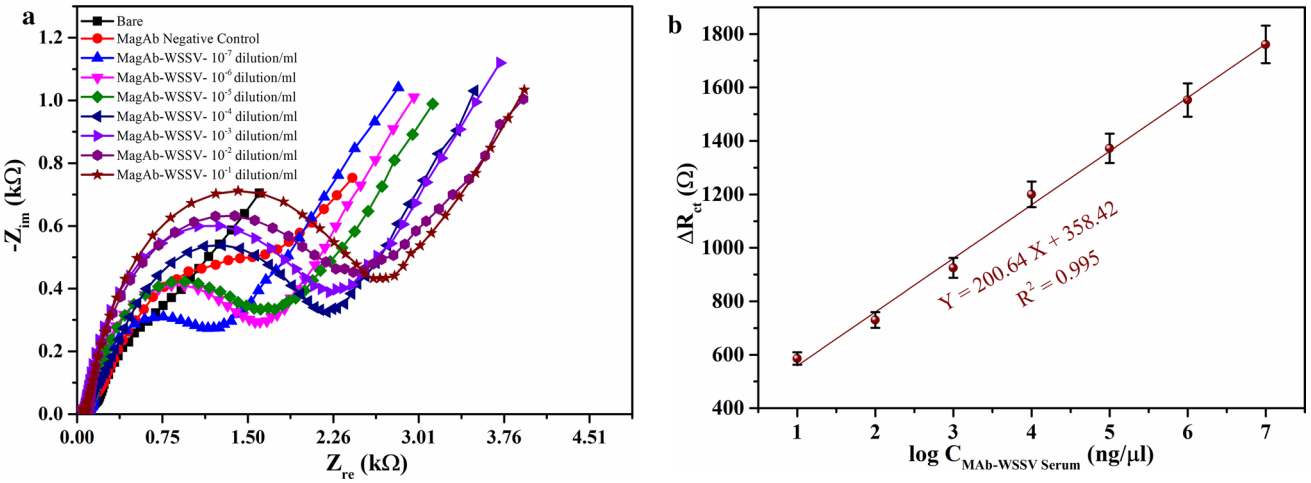

Fig. 8 **a** Detection of WSSV using magnetosome-VP28 antibody (0.025 ng/µl) complex, **b** Linear plot for WSSV detection

an increase in the R_{CT} value was observed as the SPCE was modified with various dilutions of WSSV (10^{-7} to 10^{-1}) interacting with magnetosome-VP28 antibody complex (10^{-7}, 982 Ω; 10^{-6}, 1126 Ω; 10^{-5}, 1321 Ω; 10^{-4}, 1596 Ω; 10^{-3}, 1768 Ω; 10^{-2}, 1949 Ω; 10^{-1}, 2157 Ω). This indicates that the magnetosome-VP28 antibody complex interacted with WSSV. The linear fit had an R^2 value of 0.0995. The values obtained for the different modifications of the equivalent circuit are shown in Table 5.

Western blot and RT-PCR analysis

Western blotting was done to confirm the presence of VP28 antigen in infected samples. The western blot showed sharp VP28 bands on the first and seventh days postinfection, indicating the presence of VP28 antigen in the infected samples (Fig. 9a).

VP28-specific primers (VP28-Rt–PCR) were used for reverse transcription (RT-PCR), and an amplicon of the expected size was produced, indicating the presence of WSSV in the infected crabs (Fig. 9b).

Cross-reactivity assay

A cross-reactivity assay was performed to examine the reactivity of the VP28 antibody with non-VP28 antigens. The VP28 antibody bound efficiently with VP28 antigen (0.862), while non-VP28 antigens, namely LC and EHP, exhibited negligible reactivity (0.005). IHNVV exhibited minimum reactivity (0.08), while ET exhibited no reactivity with VP28 antibody (Fig. 10a). This confirms that the VP28 antibody is specific for the VP28 antigen.

The magnetosome-VP28 antibody showed negligible to low resistance with control and other seafood pathogens (ET,

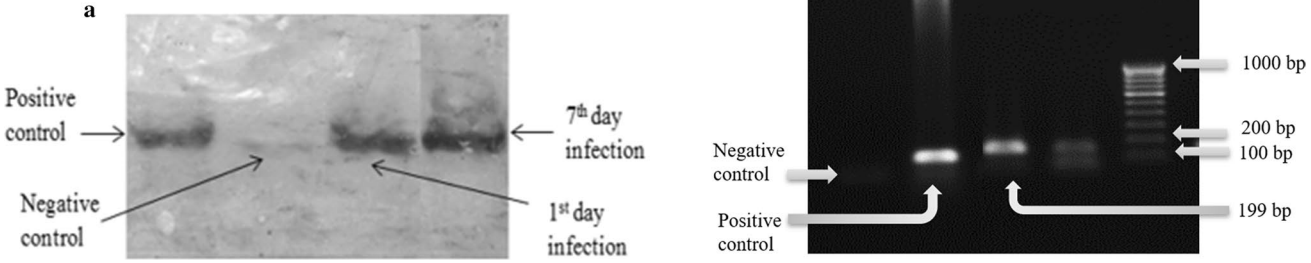

Fig. 9 **a** Western blot of WSSV-infected samples. In comparison with the positive control, the amount of viral protein was higher 7 days postinfection than 1 day postinfection. **b** RT-PCR amplification of the VP28 gene from samples obtained from the head and gills, indicating the presence of WSSV in the infected crabs

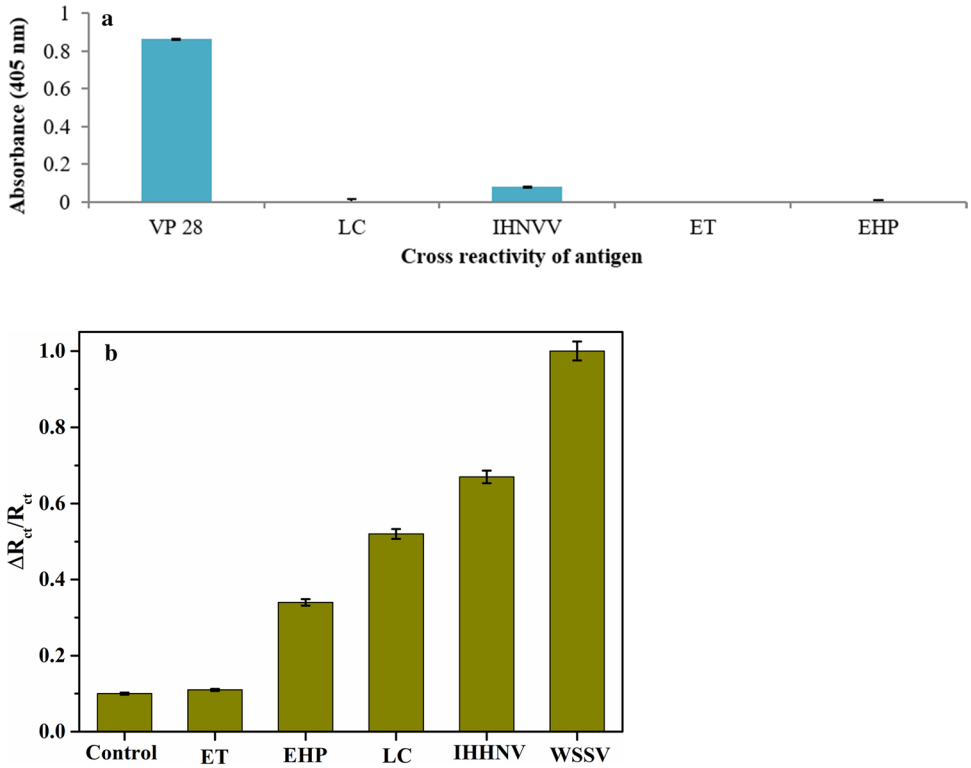

Fig. 10 **a** Colorimetric-based cross-reactivity. **b** Impedance-based cross-reactivity

LC, EHP, IHNVV) when compared with the positive samples of WSSV (Fig. 10b). This indicates the specificity of the magnetosome-VP28 antibody-based biosensor (Table 6).

Discussion

Magnetosomes, with their numerous applications in nanobiotechnology and drug delivery, could bring new advances in nanoscience, and new challenges in biotechnology have allowed us to exploit their potential. In the current study, we have investigated the commercial aspect of magnetosomes and their role in the development of biosensors to detect WSSV in a cost-effective, sensitive, and rapid manner. The magnetosomes were extracted from *Magnetospirillum* sp. RJS-1 [34], a novel strain that is capable of producing more magnetosomes than the previously reported strains [43].

Magnetosomes are widely known to have advantages over other types of nanoparticles [43, 44]. Moreover, the magnetic entity in magnetosomes plays a key role in therapeutics and diagnostics [45, 46]. Advances in nanobiotechnology have facilitated innumerable applications based on unique biomolecular interactions [47, 48]. However, nanoparticles are restricted by their chemical composition, requiring the use of linkers such as biotin, streptavidin, and glutaraldehyde [49–51]. In 2015, an immunomagnetic reduction assay was developed in which chemically synthesized magnetic nanoparticles were conjugated to antibodies via linkers for the detection of WSSV [52]. Our study differs from the previous report by Liu et al. [52], as we have implemented the use of

Table 6 Impedance response for various dilution of WSSV interacting with magnetosome-VP28 antibody complex

Concentration of MagAb-WSSV	R_S (Ω)	C_{dl} (μF)	R_{CT} (Ω)	Q	W (Ω)	RSD%
Bare	205	1.84	396	0.81	1.08×10^{-5}	2.64
MagAb negative control	196	2.03	850	0.98	1.24×10^{-5}	1.98
MagAb-WSSV 10^{-7} dilution	178	2.25	982	0.73	2.35×10^{-5}	2.54
MagAb-WSSV 10^{-6} dilution	193	2.43	1126	0.86	2.54×10^{-5}	2.06
MagAb-WSSV 10^{-5} dilution	205	2.69	1321	0.62	2.79×10^{-5}	1.78
MagAb-WSSV 10^{-4} dilution	198	2.86	1596	0.75	2.92×10^{-5}	2.67
MagAb-WSSV 10^{-3} dilution	204	2.99	1768	0.89	3.09×10^{-5}	2.98
MagAb-WSSV 10^{-2} dilution	206	3.14	1949	0.84	3.21×10^{-5}	3.11
MagAb-WSSV 10^{-1} dilution	196	3.28	2157	0.96	3.34×10^{-5}	3.29

magnetosomes containing biological membranes that bind directly to antibodies without any linkers. Moreover, their genetically controlled biological synthesis allows magnetosomes to have various unique properties, including linear chains, dipole moment, biocompatibility, better dispersity in solution, and thermal stability, that give them an advantage over magnetic nanoparticles [53].

The magnetosomes were bound directly to the VP28 antibody, as indicated by the higher absorbance of the magnetosome-VP28 antibody complex detected by spectroscopy. Arakaki et al. [54] also hypothesized the direct binding of magnetosomes to antibodies, as it could strengthen the binding kinetics and affinity of both biomolecules. The binding of VP28 antigen with the magnetosome-VP28 complex was also confirmed by absorbance measurements.

Antibody-antigen interactions were analyzed by ELISA. Various concentrations of magnetosome-VP28 antibody complex, VP28 antibody, and VP28 antigen were tested to optimize the assay. VP28 antibody conjugated to magnetosomes had 75% higher reactivity in ELISA than VP28 antibody alone. Lakshmipriya et al. [55] reported signal enhancement in ELISA when gold nanoparticles were used. Similarly, enzymes such as glucose oxidase have been shown to give 40-fold higher reactivity when bound to artificial magnetite [56]. It has also been reported that the antibodies have stronger reactivity when immobilized on magnetosomes, [57]. In our study, the activity of VP28 antibody was enhanced in the presence of magnetosomes for the detection of VP28 antigen. Yi et al. [10] used a 0.05 ng/μL concentration of VP28 antibody in ELISA, which was 50% higher than the concentration of VP28 antibody used in our study. Other studies have used a very high concentration of VP28 antibody (25 μg/mL) for conjugation with nanoparticles, but we have optimized the concentration of VP28 antibody to a minimum concentration (0.025 ng/μl), which reduces the cost of the assay [58].

The lowest concentration of VP28 antigen detected in ELISA was 0.025 ng/μl. However, the detection limit of VP28 antigen in ELISA with magnetosomes was 75% lower than in the traditional ELISA. Past reports have shown a high detection limit of VP28 antigen (100 μg/ml and 100 ng/ml) in ELISA [10, 58].

The easy storage of the magnetosome-VP28 antibody conjugates and simple modification of classical makes the magnetosome-based assay a practical alternative. An ELISA using magnetosomes was used to test infected tissue samples, showing that the magnetosome-VP28 antibody complex can directly detect VP28 antigen in tissue samples within 24 h.

We have further simplified the assay so that it can be easily performed by non-professionals by using a sensor. Electrochemical impedance spectroscopy (EIS) is a powerful technique to analyze interfacial electron transfer characteristics and to determine kinetic parameters such as R_{CT} and association-disassociation kinetics of biological complexes at the modified electrode surface. A previous study showed the development of a biosensor using gold electrodes that focused on antibody-antigen interaction for the rapid detection of WSSV [59]. Although the method used in that study allows rapid detection of WSSV, the high cost of gold electrodes is a disadvantage [60]. The recent development of disposable SPCEs has allowed them to replace traditional electrodes for various applications [61]. They can be used in disposable devices due to their low cost while also providing sensitive and selective analysis [62]. Moreover, SPCEs require low sample volume, which allows different types of samples to be tested.

Since magnetosomes were found to enhance the reactivity of the VP28 antibody, further electrochemical analysis based on SPCEs was performed with magnetosome-VP28 antibody complexes to detect the VP28 antigen and WSSV. The magnetosome-VP28 antibody complex was easily concentrated on the SPCE using an external magnetic field and various concentrations of VP28 antigen (0.01-1 ng/μl) were measured. The SPCE provides a platform for convenient separation of the virus through magnetic-based separation [62]. The magnetosome-VP28 antibody complex-based sensor was able to detect WSSV (10^{-1} to 10^{-7} dilution) in homogenized crab sample.

In certain cases, antibodies show cross-reactivity with nonspecific antigens, resulting in false-positive results [63, 64]. Therefore, the specificity of the biosensor was verified using non-VP28 antigens. The impedimetric-based magnetosome-coupled biosensor is the first of its kind in which user-friendly screen-printed carbon electrodes were used to detect small amounts of VP 28 antigen and WSSV.

The biosensor was effective in detecting the VP28 antigen and WSSV. The small volume and concentration of magnetosome-VP28 antibody complex needed for electrochemistry make this technique more efficient than western blot and PCR. Although PCR has been extensively used for the detection of WSSV in tissue samples, it is very time-consuming, and the wide range of primers used during the process make it an expensive procedure [65]. The real-time PCR analysis of WSSV-infected sample allows 1.37×10^7 copies/μl in a 50 mg of tissue sample to be detected [66]. However, in our study, the tissue sample could be diluted further (10^{-7}) to detect the presence of WSSV within 30 min using a magnetosome-antibody-based biosensor with a working volume of 15 μl. The sensor demonstrated a consistent decrease in the charge transfer resistance with increasing dilution. A linear plot with $R^2 = 0.099$ for WSSV detection verified the consistency of the data.

The magnetosome-based biosensor described here is effective for detecting the VP28 antigen as well as WSSV in seafood samples. It provides a simple and rapid assay that can

be performed easily within 30 min, in contrast to the established methods, which take 24-48 hours. Moreover, owing to the benefits of SPCEs, the magnetosome-antibody complex-immobilized SPCEs could be easily available for 200-300 INR for a WSSV test, compared to the current established methods, e.g., WSSV detection kit (Genei) for 15,050-34,548 INR [67]. The ability to use a small volume of sample (15 µl) and concentration of the magnetosome-antibody complex also reduces the cost of the overall process. SPCEs are easily produced in bulk quantity and are compatible with a large number of devices and instruments [62]. The established model could be further implemented using various other seafood samples for future applications. Further development of this biosensor could provide us with portable devices that could be handled easily by individuals.

Conclusions

The implementation of magnetosomes in ELISA produced a 75% cost-effective and sensitive method to detect the VP28 antigen. The magnetosome-coupled VP28 antibody was efficient in detecting a low concentration of VP28 antigen in WSSV-infected seafood samples. The magnetosome-VP28 antibody complex was easily immobilized on SPCEs. The sensitive, rapid, and specific detection of VP28 antigen and WSSV was demonstrated in electrochemical studies. The presence of VP28 antigen in infected samples was also confirmed by western blotting and RT-PCR.

Acknowledgements This study was funded by a Grant-in-Aid from the Department of Biotechnology (DBT-No. BT/PR10570/PFN/20/839/2013).

Author contributions SS performed the experiments and prepared the manuscript. SKA performed the electrochemical part, JM supervised the electrochemical part. RS supervised the VP28 extraction part. SK supervised the experiments described in the article. All authors approved the final draft.

Funding Funded by the Department of Biotechnology (DBT-No. BT/PR10570/PFN/20/839/2013).

Availability of data and materials The datasets in the current study are available from the corresponding author on request.

Declarations

Conflict of interest All authors declare no conflict of interest.

Ethical approval No humans or animals were used in this study.

References

1. Guoxing Z, Yalin S, Kai Z, Zhi C (1997) Bacilliform virus infection in cultured Chinese shrimp, *Penaeus orientalis*, in China. J Mar Biotechnol 5:113–118
2. Sánchez-Paz A (2010) White spot syndrome virus: an overview on an emergent concern. Vet Res 41(6):43. https://doi.org/10.1051/vetres/2010015
3. Inouye K, Miwa S, Oseko N, Nakano H, Kimura T, Momoyama K, Hiraoka M (1994) Mass mortalities of cultured kuruma shrimp, *Penaeus japonicus*, in Japan in 1993: electron microscopic evidence of the causative virus. Fish Pathol 29:149–158. https://doi.org/10.3147/jsfp.29.149
4. Takahashi Y, Itami T, Kondo M, Maeda M, Fujii R, Tomonaga S, Supamattaya K, Boonyaratpalin S (1994) Electronmicroscopic evidence of bacilliform virus infection in Kuruma Shrimp (*Penaeus japonicus*). Fish Pathol 29(2):121–125. https://doi.org/10.3147/jsfp.29.121
5. Lo CF, Ho CH, Peng SE, Chen CH, Hsu HC, Chiu YL, Chang CF, Liu KF, Su MS, Wang CH, Kou GH (1996) White spot syndrome baculovirus (WSBV) detected in cultured and captured shrimp, crabs and other arthroponds. Dis Aquat Org 27:215–225. https://doi.org/10.3354/dao027215
6. Karunasagar I, Otta SK, Karunasagar I (1997) Histopathological and bacteriological study of white spot syndrome of *Penaeus monodon* along the west coast on India. Aquaculture 153:9–13. https://doi.org/10.1016/S0044-8486(97)00011-2
7. Chou HY, Huang CY, Wang CH, Chiang HC, Lo CF (1995) Pathogenicity of a baculovirus infection causing white spot syndrome in cultured penaeid shrimp in Taiwan. Dis Aquat Org 23:165–173. https://doi.org/10.3354/dao023165
8. Li LJ, Yuan JF, Cai CA, Gu WG, Shi ZL (2006) Multiple envelope proteins are involved in white spot syndrome virus (WSSV) infection in crayfish. Arch Virol 151(7):1309–1317. https://doi.org/10.1007/s00705-005-0719-2
9. van Hulten MCW, Witteveldt J, Peters S, Kloosterboer N, Tarchini R, Fiers M (2001) The white spot syndrome virus DNA genome sequence. Virology 286:7–22. https://doi.org/10.1006/viro.2001.1002
10. Yi G, Wang Z, Qi Y, Yao L, Qian J, Hu L (2004) VP28 of shrimp white spot syndrome virus is involved in the attachment and penetration into shrimp cells. J Biochem Mol Biol 37:726–734. https://doi.org/10.5483/BMBRep.2004.37.6.726
11. Mathew S, Kumar KA, Anandan R, Nair PV, Devadasan K (2007) Changes in tissue defence system in white spot syndrome virus (WSSV) infected *Penaeus monodon*. Comp Biochem Physiol C Toxicol Pharmacol 145(3):315–320. https://doi.org/10.1016/j.cbpc.2007.01.001
12. Oakey J, Smith C, Underwood D, Afsharnasab M, Alday-Sanz V, Dhar A, Sivakumar S, Hameed AS, Beattie K, Crook A (2019) Global distribution of white spot syndrome virus genotypes determined using a novel genotyping assay. Arch Virol 164(8):2061–2082. https://doi.org/10.1007/s00705-019-04265-2
13. Shyam SS, Geetha R, Athira NR (2019) Economic recession and Indian seafood exports: reflections and paradigms. Indian J Econ Dev 71(12):1–9. http://ijed.informaticspublishing.com/index.php/ijed/article/view/147619/104552
14. Shen CF, Meghrous J, Kamen A (2002) Quantitation of baculovirus particles by flow cytometry. J Virol Methods 105(2):321–330. https://doi.org/10.1016/S0166-0934(02)00128-3
15. Wongprasert K, Sangsuriya P, Phongdara A, Senapin S (2007) Cloning and characterization of a caspase gene from black tiger shrimp (*Penaeus monodon*)-infected with white spot syndrome virus (WSSV). J Biotechnol 131(1):9–19. https://doi.org/10.1016/j.jbiotec.2007.05.032

16. Liu W, Wang TY, Tian SD, Yin CZ, Kwang J (2002) Detection of white spot syndrome virus (WSSV) of shrimp by means of monoclonal antibodies (MAbs) specific to an envelope protein (28 kDa). Dis Aquat Org 49:11–18. https://doi.org/10.3354/dao049011
17. Song KK, Li DF, Zhang MC, Yang HJ, Ruan LW, Xu X (2010) Cloning and characterization of three novel WSSV recognizing lectins from shrimp *Marsupenaeus japonicus*. Fish Shellfish Immunol 28(4):596–603. https://doi.org/10.1016/j.fsi.2009.12.015
18. Wang L, Zhi B, Wu W, Zhang X (2008) Requirement for shrimp caspase in apoptosis against virus infection. Dev Comp Immunol 32(6):706–715. https://doi.org/10.1016/j.dci.2007.10.010
19. Xie Z, Xie L, Pang Y, Lu Z, Xie Z, Sun J, Deng X, Liu J, Tang X, Khan M (2008) Development of a real-time multiplex PCR assay for detection of viral pathogens of penaeid shrimp. Arch Virol 153(12):2245–2251. https://doi.org/10.1007/s00705-008-0253-0
20. Sithigorngul W, Rukpratanporn S, Pecharaburanin N, Longyant S, Chaivisuthangkura P, Sithigorngul P (2006) A simple and rapid immunochromatographic test strip for detection of white spot syndrome virus (WSSV) of shrimp. Dis Aquat Org 72:101–106. https://doi.org/10.3354/dao072101
21. Fitzpatrick J, Fanning L, Hearty S, Leonard P, Manning BM, Quinn JQ, O'Kennedy R (2000) Applications and recent developments in the use of antibodies for analysis. Anal Lett 33(13):2563–2609. https://doi.org/10.1080/00032710008543210
22. Killard AJ, Smyth MR (2000) Separation-free electrochemical immunosensor strategies. Anal Lett 33(8):1451–1465. https://doi.org/10.1080/00032710008543135
23. Zhang S, Wang N, Yu H, Niu Y, Sun C (2005) Tailoring the surface potential of gold nanoparticles with self-assembled monolayers with mixed functional groups. Biochemistry 67:15–22. https://doi.org/10.1016/j.jcis.2009.08.014
24. Luo X, Morrin A, Killard Anthony J, Smyth Malcolm R (2006) Application of nanoparticles in electrochemical sensors and biosensors. Electroanalysis 18(4):319–326. https://doi.org/10.1002/elan.200503415
25. Hussain MS, Hess LK, Gearhart MJ, Geiss TK, Schlager JJ (2005) In vitro toxicity of nanoparticles in BRL 3A rat liver cells. Toxicol In Vitro 19:975–983. https://doi.org/10.1016/j.tiv.2005.06.034
26. Salata OV (2004) Applications of nanoparticles in biology and medicine. J Nanobiotechnol 2(1):1. https://doi.org/10.1016/j.msec.2020.111071
27. Banerjee SK, Moskowitz BM (1985) Ferrimagnetic properties of magnetite. In: Kirschvink JL, Jones DS, MacFadden BM (eds) Magnetite biomineralization and magnetoreception in organisms. Plenum Press, New York and London, pp 17–41
28. Bazylinski AD, Garratt-Reed JA, Frankel BR (1994) Electron microscopic studies of magnetosomes in magnetotactic bacteria. Microsc Res Tech 27(5):389–401. https://doi.org/10.1002/jemt.1070270505
29. Nakamura N, Matsunaga T (1993) Highly sensitive detection of allergen using bacterial magnetic particles. Anal Chim Acta 281:585–589. https://doi.org/10.1016/0003-2670(93)85018-F
30. Frankel RB, Bazylinski DA, Schueler D (1998) Biomineralization of magnetic iron minerals in bacteria. Supramol Sci 5:383–390. https://doi.org/10.1016/S0968-5677(98)00036-4
31. Winklhofer M, Petersen N (2000) Paleomagnetism and magnetic bacteria. Magnetoreception and magnetosomes in bacteria. Springer, Berlin Heidelberg, pp 255–273
32. Matsunaga T, MaedaY YT, Takeyama Harumi Ginya J, Aasahina T, Sakaguchi T, Tadokoro F (1991) Magnetite formation by a magnetic bacterium capable of growing aerobically. Appl Microbiol Biotechnol 35:651–655. https://doi.org/10.1007/BF00169632
33. Matsunaga T, Okamura Y (2002) Molecular mechanism of bacterial magnetite formation and its application. Mat Res Soc Symp Proc 724:11–24. https://doi.org/10.1557/PROC-724-N1.4
34. Revathy T, Jacob JJ, Jayasri MA, Suthindhiran K (2016) Isolation and characterization of *Magnetospirillum* from saline lagoon. World J Microbiol Biotechnol 32:109. https://doi.org/10.1007/s11274-016-2075-7
35. Sannigrahi S, Arumugasamy SK, Mathiyarasu J, Suthindhiran K (2020) Magnetosome-anti-Salmonella antibody complex based biosensor for the detection of *Salmonella typhimurium*. Mater Sci Eng C. https://doi.org/10.1016/j.msec.2020.111071
36. Hameed AS, Yoganandhan K, Sathish S, Rasheed M, Murugan V, Jayaraman K (2001) White spot syndrome virus (WSSV) in two species of freshwater crabs (*Paratelphusa hydrodomous* and *P. pulvinata*). Aquaculture 201(3–4):179–186. https://doi.org/10.1016/S0044-8486(01)00525-7
37. Dinesh S, Karmarkar M, Vinodhini S, Vidhya G, Hemalatha K, Sudhakaran R (2014) Confirmation of Anti-WSSV activity from Red Algae *Hypnae spinella* in freshwater crab *Paratelphusa hydrodomous*. Int J ChemTech Res 6(8):4022–4026
38. Hameed AS, Balasubramanian G, Musthaq SS, Yoganandhan K (2003) Experimental infection of twenty species of Indian marine crabs with white spot syndrome virus (WSSV). Dis Aquat Org 57(1–2):157–161. https://doi.org/10.3354/dao057157
39. Lowry OH, Rosebrough NJ, Farr AL, Randall RJ (1951) Protein measurement with the Folin phenol reagent. J Biol Chem 193:265–275
40. Woo MA, Kim MI, Jung JH, Park KS, Seo TS, Park HG (2013) A novel colorimetric immunoassay utilizing the peroxidase mimicking activity of magnetic nanoparticles. Int J Mol Sci 14(5):9999–10014. https://doi.org/10.3390/ijms14059999
41. Talbot JP, Knobler LR, Buchmeier JM (1984) Western and dot immunoblotting analysis of viral antigens and antibodies: application to *Murine Hepatitis virus*. J Immunol Methods 73:177–188. https://doi.org/10.1016/0022-1759(84)90043-7
42. Reddy R, Bala C, Dinesh S, Anusha N, Itami T, Rajasekhara Reddy S, Sudhakaran R (2015) Antiviral activity of 3-(1-chloropiperidin-4-yl)-6-fluoro benzisoxazole 2 against White spot syndrome virus in Freshwater crab, *Paratelphusa hydrodomous*. Aquac Res 47(8):2677–2681. https://doi.org/10.1111/are.12704
43. Heyen U, Schüler D (2003) Growth and magnetosome formation by microaerophilic *Magnetospirillum* strains in an oxygen-controlled fermentor. Appl Microbiol Biotechnol 61(5–6):536–544. https://doi.org/10.1007/s00253-002-1219-x
44. Jacob JJ, Suthindhiran K (2016) Magnetotactic bacteria and magnetosomes—scope and challenges. Mater Sci Eng C 68:919–928. https://doi.org/10.1016/j.msec.2016.07.049
45. Long RM, Dai QL, Zhou X, Cai DH, Hong YZ, Wang SB, Liu YG (2018) Bacterial magnetosomes-based nanocarriers for co-delivery of cancer therapeutics in vitro. Int J Nanomed 13:8269. https://doi.org/10.2147/IJN.S180503
46. Boucher M, Geffroy F, Prévéral S, Bellanger L, Selingue E, Adryanczyk-Perrier G, Pean M, Lefèvre CT, Pignol D, Ginet N, Mériaux S (2017) Genetically tailored magnetosomes used as MRI probe for molecular imaging of brain tumor. Biomaterials 121:167–178. https://doi.org/10.1016/j.biomaterials.2016.12.013
47. Zhang S, Moustafa Y, Huo Q (2014) Different interaction modes of biomolecules with citrate-capped gold nanoparticles. ACS Appl Mater Interfaces 6(23):21184–21192. https://doi.org/10.1021/am506112u
48. Auría-Soro C, Nesma T, Juanes-Velasco P, Landeira-Viñuela A, Fidalgo-Gomez H, Acebes-Fernandez V, Gongora R, Almendral Parra MJ, Manzano-Roman R, Fuentes M (2019) Interactions of nanoparticles and biosystems: microenvironment of nanoparticles and biomolecules in nanomedicine. Nanomaterials 9(10):1365. https://doi.org/10.3390/nano9101365

49. Lee Y, Lee S, Jon S (2018) Biotinylated bilirubin nanoparticles as a tumor microenvironment-responsive drug delivery system for targeted cancer therapy. Adv Sci 5(6):1800017. https://doi.org/10.1002/advs.201800017
50. Liu G, Lu M, Huang X, Li T, Xu D (2018) Application of gold-nanoparticle colorimetric sensing to rapid food safety screening. Sensors 18(12):4166. https://doi.org/10.3390/s18124166
51. Moghaddam AZ, Esmaeilkhanian E, Shakourian-Fard M (2019) Immobilizing magnetic glutaraldehyde cross-linked chitosan on graphene oxide and nitrogen-doped graphene oxide as well-dispersible adsorbents for chromate removal from aqueous solutions. Int J Biol Macromol 128:61–73. https://doi.org/10.1016/j.ijbiomac.2019.01.086
52. Liu BH, Lin YC, Ho CS, Yang CC, Chang YT, Chang JF, Li CY, Cheng CS, Huang JY, Lee YF, Hsu MH (2015) A novel detection platform for shrimp white spot syndrome virus using an ICP11-dependent immunomagnetic reduction (IMR) assay. PLoS ONE 10(9):e0138207. https://doi.org/10.1371/journal.pone.0138207
53. Józefczak A, Leszczyński B, Skumiel A, Hornowski T (2016) A comparison between acoustic properties and heat effects in biogenic (magnetosomes) and abiotic magnetite nanoparticle suspensions. J Magn Magn Mater 407:92–100. https://doi.org/10.1016/j.jmmm.2016.01.054
54. Arakaki A, Nakazawa H, Nemoto M, Mori T, Matsunaga T (2008) Formation of magnetite by bacteria and its application. J R Soc Interface 5(26):977–999. https://doi.org/10.1098/rsif.2008.0170
55. Lakshmipriya T, Gopinath SC, Hashim U, Tang TH (2016) Signal enhancement in ELISA: biotin-streptavidin technology against gold nanoparticles. J Taibah Univ Med Sci 11(5):432–438. https://doi.org/10.1016/j.jtumed.2016.05.010
56. Matsunaga T, Kamiya S (1987) Use of magnetic particles isolated from magnetotactic bacteria for enzyme immobilization. Appl Microbiol Biotechnol 26:328–332. https://doi.org/10.1007/BF00256663
57. Nakamura N, Burgess GJ, Yagiuda K, Kudo S, Sakaguchi T, Mataunaga T (1993) Detection and removal of *Escherichia coli* using fluorescein isothiocyanate conjugated monoclonal antibody immobilized on bacterial magnetic particles. Anal Chem 65:2036–2039. https://doi.org/10.1021/ac00063a018
58. Kulabhusan PK, Rajwade JM, Sugumar V, Taju G, Hameed AS, Paknikar KM (2017) Field-usable lateral flow immunoassay for the rapid detection of white spot syndrome virus (WSSV). PLoS ONE 12(1):e0169012. https://doi.org/10.1371/journal.pone.0169012
59. Loyprasert-Thananimit S, Saleedang A, Kanatharana P, Thavarungkul P, Chotigeat W (2012) Production of a polyclonal antibody to the VP26 nucleocapsid protein of White Spot Syndrome Virus (WSSV) and its use as a biosensor. Front Chem Sci Eng 6(2):216–223. https://doi.org/10.1007/s11705-012-1289-y
60. Pang S, Tsao HN, Feng X, Müllen K (2009) Patterned graphene electrodes from solution-processed graphite oxide films for organic field-effect transistors. Adv Mater 21(34):3488–3491. https://doi.org/10.1002/adma.200803812
61. Renedo OD, Alonso-Lomillo MA, Martinez MA (2007) Recent developments in the field of screen-printed electrodes and their related applications. Talanta 73(2):202–219. https://doi.org/10.1016/j.talanta.2007.03.050
62. Munteanu FD, Titoiu AM, Marty JL, Vasilescu A (2018) Detection of antibiotics and evaluation of antibacterial activity with screen-printed electrodes. Sensors 18(3):901. https://doi.org/10.3390/s18030901
63. Aalberse RC, Akkerdaas J, Van Ree R (2001) Cross-reactivity of IgE antibodies to allergens. Allergy 56(6):478–490. https://doi.org/10.1034/j.1398-9995.2001.056006478.x
64. Väkeväinen M, Eklund C, Eskola J, Käyhty H (2001) Cross-reactivity of antibodies to type 6B and 6A polysaccharides of *Streptococcus pneumoniae* evoked by pneumococcal conjugate vaccines, in infants. J Infect Dis 184(6):789–793. https://doi.org/10.1086/322984
65. Wu W, Wang L, Zhang X (2005) Identification of white spot syndrome virus (WSSV) envelope proteins involved in shrimp infection. Virology 332(2):578–583. https://doi.org/10.1016/j.virol.2004.12.011
66. Natarajan A, Devi KS, Raja S, Kumar AS (2017) An elegant analysis of white spot syndrome virus using a graphene oxide/methylene blue based electrochemical immunosensor platform. Sci Rep 7(1):1–11. https://doi.org/10.1038/srep46169(2017)
67. WSSV Detection Kit, http://geneilabs.com/product/wssv-detection-kit-25-tests/. Accessed 22 Mar 2021